RSC Advances

ROYAL SOCIETY OF CHEMISTRY

www.rsc.org/advances

Enhancing Photocatalytic Degradation of Phenol through Nitrogen- and Nitrogen/Fluorine-Codoped Ti-SBA-15

LiliYang[a], BinWang[a], SufengLai[a], ChongwenJiang[a] and HongZhong[a]

[a]*College of Chemistry and Chemical Engineering, Central South University, Changsha 410083, China*

Correspondence to: Chongwen Jiang, E-mail:jcwcsu@csu.edu.cn

College of Chemistry and Chemical Engineering, Central South University, Changsha 410083, China

Tel.: +86-731-88879616

Fax: +86-731-88879616

Abstract:F-N/Ti-SBA-15 and N/Ti-SBA-15 were prepared by hydrothermal method using ammonium fluoride and triethylamine as nonmetal dopants, respectively. The structure and surface properties of the as-prepared samples have been characterized by N_2 adsorption-desorption isotherms, UV-Vis DRS spectra, FT-IR and XPS. It was found that the doping of non-metals could narrow the band gap of samples without changes in the mesoporous structure properties. The F-N/Ti-SBA-15 was demonstrated as efficient catalyst for photodegradation of phenol both in the UV light and visible light. The formation of surface oxygen vacancies may be responsible for the promotion of nonmetal F-N/Ti-SBA-15 on the photodegradation of phenol.

Keywords: photocatalysis; hydrothermal method; Ti-SBA-15; non-metal-doped; phenol

1 Introduction

Due to their environmental toxicity, persistency, ubiquitous presence and carcinogenicity, the increasing pollution of phenols and other associated environmental hazards in waste water has become a serious health and environmental problem[1]. The development of methods to remove the contaminants from waste water has gained considerable interests[2]. Among them, the heterogeneous photocatalytic oxidation process using titanium dioxide has emerged with a good potential through which the complete mineralization of highly toxic phenol compounds in water can be achieved[3]. However, titanium dioxide requires UV light irradiation to obtain its photocatalytic activity because of its wide band gap (Eg=3.2 eV), leading to low utilization of visible light[4]. It is necessary to search more economical and effective photocatalyst in the visible region for application.

Recently, a great number of researches have been carried out to improve the photocatalytic activity of titanium dioxide by using a solid support to increase the amount of active sites per unit area, and achieve a higher photocatalytic reaction rate under irradiation[5]. Furthermore, many studies have demonstrated that the presence of transition metals or noble metals can improve the charge transfer and consequently the performance of the photochemical degradation process[6,7]. Nevertheless, it is argued that the doped metal ion can cause lower thermal stability and carrier-recombination. Moreover, transition metal ions doping requires expensive equipment[8]. The preparation and characteristic of nonmetal-modified titanium dioxide particles has therefore attracted much attention. Many non-metal elements such as B, C, N, S, P and F have been employed to dope into titanium dioxide and efficiently extend the photo response range from ultraviolet (UV) to visible light region. Dozzi et al.[9] synthesized F-TiO_2via a sol-gel method in the presence of NH_4F followed by calcination and found that F-TiO_2 exhibited high photocatalytic activity in the

degradation of formic acid under visible light irradiation, which was ascribed to highly crystalline pure anatase and reduced the charge carrier recombination. Yu et al.[10] proposed that F-TiO_2 synthesized using a modified sol-gel method showed enhanced photocatalytic activity(91%) in the degradation of methylene blue under visible light irradiation as compared with pure titanium dioxide(32%), arising from oxygen vacancies and Ti^{3+} surface states in F-TiO_2.Kadam et al. [11] reported solar light driven N-doped titanium dioxide photocatalyst with controlled size by microwave assisted method, indicating higher photocatalytic performance in the degradation of Malathion. Liang et al.[12] prepared B-doped titanium dioxide particles with different ratios of B to Ti by a direct hydrolysis of tetrabutyltitanate in a solution of boric acid, and Rhodamine B degradation was used as a test reaction to evaluate the photocatalytic activity of B-doped titanium dioxide under simulate sunlight.

As was stated above, there is no doubt that nonmetallic ion doping is beneficial to the photocatalytic activity for visible light. To the best of our knowledge, studies on the nonmetal doped Ti-SBA-15 are very scarce, there is no report on nonmetal doped Ti-SBA-15 to improve the photodegration of phenol in visible light. The photocatalytic reactions take place on the surface and thus the surface properties of the photocatalysts play a critical part in determining reaction efficiencies and mechanisms. However, their mechanism is still debatable. In our present work, nonmetal-doped Ti-SBA-15 with high special area was successfully synthesized by hydrothermal method. The prepared materials were characterized by N_2 adsorption-desorption isotherms, FT-IR, XPS and UV-Vis DRS, respectively. Their catalytic performance towards the photodegration of phenol under both ultraviolet and visible light was systematically evaluated.

2 Experimental

2.1 Catalyst preparation

Non-metal nitrogen doped Ti-SBA-15 or nitrogen and fluorinecodopedTi-SBA-15 were synthesized via hydrothermal method using TEOS and tetrabutyltitanate (TBT) as the sources of Si and Ti, respectively. And ammonium fluoride(NH_4F) and triethylamine（$(CH_3CH_2)_3N$）were used as nonmetal dopants.

In a typical synthesis, 4.0 g of pluronic P123 was completely dissolved in 146.7 g distilled water and 6.7mL hydrochloric acid (37wt. %) under stirring at room temperature. Thereafter, 8.7 g TEOS was dripped into the solution and stirred for 2 h.1.4 g of TBT in 10mL ethanol was slowly added to the acid solution under vigorous stirring at 38℃. Next, a corresponding amount of ammonium fluoride, which the molar ratio of F and N to Ti is 0.5, 1 and 2, respectively, was added into it. After stirring for 20 h, the resultant mixture was transferred into a polypropylene bottle and aged at 100℃ for another 20h without stirring. The resulting mixtures were filtered and washed to remove unreacted nonmetal doping agent with distilled water. The residue was dried at 100℃for 12 h and finally calcinated at 550℃ for 5 h in air to obtain the N and F co-doped Ti-SBA-15 mesoporous products denoted as N-F/Ti-SBA-15.

N/Ti-SBA-15 was synthesized following the same procedure except that the non-metal dopant was triethylamine.

2.2 Catalyst characterization

Diffuse reflectance UV-Vis DRS spectra was recorded in the range of 200-800 nm at room temperature by a Shimadzu UV-2450A double-beam digital spectrophotometer with $BaSO_4$as reference. FT-IR spectra of the samples were measured using an AVATAR-360 spectrometer. Nitrogen adsorption-desorption isotherms were obtained using a Micromeritics ASAP 2020 Gas Adsorption Analyzer at 77K after the mesoporous materials were degassed in vacuum at 200 ℃ for 5 h. Surface area and total pore volume were determined by using the Brunauer-Emmett-Teller (BET) equation and the Barrett-Joyner-Halenda (BJH) method, respectively. The pore size

distribution was calculated from the analysis of the adsorption branch of the nitrogen isotherm using the BJH method. XPS analysis was performed on ESCALAB 250Xi type of X-ray photoelectron spectrometer produced by ThermoFisher-VG Scientific.

2.3 Photocatalytic properties of the samples

To evaluate the photocatalytic properties of the samples, photocatalytic reaction experiment was performed in a batch of glass reactor. 200 ml phenol solution (100 mg/L) as a model compound was added to the glass reactor in the presence of hydrogen peroxide and nonmetal modified Ti-SBA-15 (0.2 g). A 250 W medium pressure mercury lamp (365 nm) and a 300 W xenon lamp fixed with an UV filter were used as ultraviolet light and simulated visible light, respectively. The adsorption equilibrium experiment was carried out for 30 min before illumination in order to avoid the effect of the surface adsorption. To determine the concentrations of phenol solution during the process, 5 ml of the solution from the reaction mixture was taken, subsequently centrifuged, and filtered through a millipore filter to obtain the filtrate for concentration determination by using 4-Aminoantipyrine spectrophotometric method[13]. The phenol concentration was calculated from the absorbance at 510 nm using a calibration curve.

3 Results and discussion

3.1 Characterization of samples

XRD patterns of N/Ti-SBA-15 (N/Ti=2, molar ratio), F-N/Ti-SBA-15(F-N/Ti=2,molar ratio) and Ti-SBA-15 are shown in Fig. 1.All samples exhibit very similar patterns where three well resolved diffraction peaks corresponding to reflections of(100), (110), and (200) planes of a 2-Dhexagonal structure[14]. However, a slightly lower intensity of the peak was observed for N/Ti-SBA-15 and F-N/Ti-SBA-15, indicating the decrease crystallinity and order degree due to the doped nitrogen and fluorine.

The N_2 adsorption-desorption measurement was performed to elucidate the changes in the surface area, pore size distribution as well as pore volume. Fig. 2 gives the N_2 adsorption-desorption isotherm of Ti-SBA-15, N/Ti-SBA-15 (N/Ti=2, molar ratio) and F-N/Ti-SBA-15 (F-N/Ti=2, molar ratio) at 77 K. The typical type IV isotherm is observed with large type H1 hysteresis loops at high relative pressure (p/p_0 =0.6-0.8). The sharpness of steps also displays typical ordered mesoporous materials prepared with larger pore sizes. And significant adsorption platforms indicate ordered pore structure regularity[14].The results are consistent with on previous XRD analysis, confirming the doping of non-metal atoms has no obvious impact on mesoporous feature of samples. The pore size distribution curve of each sample is also shown in Fig. 3, and the results from the analysis of these isotherms were summarized in Table 1. The BJH pore size distribution curves of Ti-SBA-15 presents more narrow pore size distribution compared to N/Ti-SBA-15 and F-N/Ti-SBA-15, showing the uniformity of pore size was decreased by dopant of nitrogen and fluorine. Additionally, the pore size of F-N/Ti-SBA-15 significantly increases from 5.49 nm to 14.21 nm. This can be explained that the fluoride ions hydrolyze TEOS by a nucleophilic attack to form large oligomers, leading to thinner silica walls and larger pores of calcined F-N/Ti-SBA-15[15,16].

Shown in Fig. 4 are the UV-Vis DRS spectra of Ti-SBA-15 and N/Ti-SBA-15. After adding nitrogen into the samples, a clear red shift is observed and samples exhibited stronger visible light absorptions than Ti-SBA-15. And the red shift slightly increased with the increasing of doped nitrogen. The forbidden band width of Eg（≈2.93 eV）of samples can be obtained by light absorption curve according to the following formula(1)[17]:

$$E_g = \frac{1240}{\lambda_{th}} \qquad (1)$$

Where λ_{th} is the limiting wave length of titanium dioxide of light absorption.

As can be seen from the above analysis, the band gap decreased and the light response range of

samples can be extended to the visible region after nitrogen was doped, leading to the photocatalytic activity of the N/Ti -SBA-15 in visible light.

Fig. 5 presents UV-Vis DRS spectra of F-N/Ti-SBA-15 with different N-F contents. The light absorption properties of Ti-SBA-15 doped with N-F was enhanced. Compared with Ti-SBA-15, samples doped with fluorine appeared a little bit of red shift between 350-400 nm. Upon this phenomenon, Yu et al[18] pointed out that Ti^{3+} is easily generated with the help of F^- ions replacing with O^{2-} ions in the lattice in the light irradiation, which could narrow the band gap (Eg≈3.0eV) and enhance the light absorption [10]. However, several literatures[19,20] reported that there was no apparent differences in optical absorption properties between fluorine modified titanium dioxide and pure titanium dioxide. The reason may be that we used NH_4F as fluorine source in the synthesis process, the simultaneous incorporation of N with F induced the red shift of UV-Vis DRS spectra of samples[21], and the greater degree of the red shift with increasing of N and F content.

The FT-IR spectra of F-N/Ti-SBA-15 (N-F/Ti=2, molar ratio)and N/Ti-SBA-15 (N/Ti=2, molar ratio) and Ti-SBA-15 prepared are shown in Fig. 6. Generally, the broad band at 3430 cm^{-1} and narrow band at 1628 cm^{-1} attributed to stretching vibration and bending vibration of O-H in the sample surface water or hydroxyl groups[22]. The band at 962 cm^{-1} is characteristic of the Ti-O-Si vibration[23]. As to the FT-IR spectra of N/Ti-SBA-15, the peaks at 1628 cm^{-1} and 3430 $cm^{-1}$are slightly weaken ascribing to the hybrid stretching vibration and bending vibration of N-H in amine and O-H, respectively. In addition, the peak at 1474 cm^{-1} belonged to bending vibration of the Ti-N bond[24]. As can be seen, the band near 920 cm^{-1} belonged to stretching vibration of Ti-F bonds in F-N/Ti-SBA-15, illustrating F ion formed chemical bond with Ti^{4+} in a certain way[25,26].

The XPS spectra of N/Ti-SBA-15 samples recorded are also shown in Fig.7 (A-C).The N 1s spectra show a clear peak at 400.3eV, which represents the Ti-O-N bond[27,28]. And the Ti 2p spectra

of N/Ti-SBA-15 and Ti-SBA-15 consist of two peaks at approximately 460.3 eV (Ti 2p3/2) and 466 eV (Ti 2p1/2), which was attributed to Ti^{4+} incorporated into the support of molecular sieve framework[29], further confirming the incorporation of nitrogen into Ti-SBA-15.

Fig. 8 presents (A) XPS survey spectra, (B) N1s XPS spectrum, (C) F1s XPS spectrum of the F-N/Ti-SBA-15, (D) Ti2p XPS spectra of Ti-SBA-15 and the F-N/Ti-SBA-15. The sample of F-N/Ti-SBA-15 contains predominantly Ti, O, C, F and N elements. The peaks of 459 eV, 530 eV, 400 eV, 685 eV and 285 eV correspond to the binding energies of Ti 2p, O 1s, N 1s, F 1s and C 1s, respectively. And the C1sXPS peak located at around 285 eV is mainly due to carbon-based contaminant existing in the XPS instrument or the residues of the hydrolysis of tetrabutyltitanate. The peak of N1s XPS spectrum at about 399.6 eV is attributed to the nitrogen replacing oxygen in the form of O-Ti-N and the peak at 402.4 eV emerges from the intersectional N and oxidized states such as Ti-O-N[30,31]. The F 1s spectrum gives three peaks centered at 686.9eV, 683.6eV and 687.5 eV, respectively. The stronger peak centered at 687.5 eV is mainly due to the doped F atoms in TiO_2 crystal lattice, i.e. the substitute F atoms that occupied oxygen sites in the TiO_2 crystal lattice. And the F1s peak at 686.9eV, 683.6 eV is due to the surface fluoride (≡Ti-F) formed by ligand exchange reaction between F- and the surface hydroxyl group on the surface of TiO_2[32,33], which is consistent with the result of FT-IR spectra.

3.2 Photocatalytic activity of catalysts

Fig. 9 is the efficiency of photocatalytic degradation of phenol on modified Ti-SBA-15 with nitrogen. All the adsorption and photodegradation data were average value of three times repeated tests. And the largest standard deviation of adsorption and photodegradation data was 1.17%. As depicted in Fig. 9A, catalytic efficiency of nitrogen doped samples was improved obviously, which reached 73.72% under visible light irradiation for 2 h. It was thought that some O atoms in titanium

dioxide lattice were substituted by nitrogen atoms, forming a localized narrow band above the valence band (VB) with lower energy absorption of visible light. However, its catalytic performance decreases under ultraviolet light, mainly due to different catalytic mechanism. Visible light only excites electrons in the narrow band while UV light can excite electrons in the valence band and the independent narrow band[21].We also found that the degradation efficiency increases with the increase amount of nitrogen in our study. Theoretically, there is an optimum doping amount because oxygen vacancies increases with the doping amount increase, but excessive oxygen vacancies will promote recombination of the photo generated holes and electrons.

Fig.10 shows the results of the photocatalytic degradation of phenol over F-N/Ti-SBA-15 under ultraviolet or visible light irradiation for certain time. It was found that the photocatalytic activity was greatly enhanced after fluorine doping under visible light, the degradation rate of phenol can be reached 86.27% for 2 h irradiation in the presence of F-N/Ti=1. And its photocatalytic activity didn't decrease under UV light. Especially, F-N/Ti-SBA-15 possesses higher photocatalytic activity compared to N/Ti-SBA-15 with identical doping amount. The possible reason is that fluoride ion radius(0.133 nm) is relatively close to that of the oxygen ion(0.132 nm) and F was doped into the titanium silicon mesoporous molecular sieve in place of oxygen atom, thus N-F-doped titanium dioxide can generate surface oxygen vacancies in the lattice of Ti-SBA-15[18, 34] .Moreover, according to literatures reported [35] ,surface fluorinated semiconductor photocatalysts may have a significant influence on the photocatalytic processes occurring at the water-semiconductor interface. Surface F-TiO_2 could be generated via simple ligand exchange between surface hydroxyl groups on titanium dioxide and fluoride ions in water as Eq. (2). There is no adsorption between ≡Ti-F and ·OH generated by the reaction of photo

generated holes and hydroxyl radicals, thus forming free hydroxyl radicals (Eq. (3)). And free hydroxyl radicals are more conducive to photoreaction than bound hydroxyl radicals. As a result, the photocatalytic performance was enhanced by surface fluorination (Eq. (4)).

$\equiv Ti\text{-}OH + F^- \rightarrow \equiv Ti\text{-}F + OH^- pK_F=6.2$ (2)

$\equiv Ti\text{-}F + OH^-（H_2O）+ h+ \rightarrow \equiv Ti\text{-}F+ \cdot OH_{free} + H^+$(3)

$Phenol+\cdot OH_{free} \rightarrow$ products (4)

4. Conclusions

Non-metal (N, F) doped Ti-SBA-15 were successfully synthesized via hydrothermal method. Based on a series of characterization, we found UV-Vis DRS spectra of as prepared samples displays red shift, which benefits to the photocatalytic activity in the visible light. F-N/Ti-SBA-15 forms new chemical bonds of Ti-F or Ti-N confirming F and N atoms were introduced into TiO_2 crystal lattice. In comparison with non-dopedTi-SBA-15, the photocatalytic activity of Ti-SBA-15doped with F or N was remarkably enhanced under visible light. In addition, F-N/Ti-SBA-15 shows higher performance, and the degradation rate of phenol is 86.27% under visible light for 2 h without obvious decreasing of the activity in the ultraviolet. The formation of surface oxygen vacancies may be responsible for the promotion of nonmetal F-N/Ti-SBA-15 on the photodegradation of phenol.

Acknowledgements

The authors thank the China-Japan International Cooperation Project (2013DFG50150) and the National Natural Science Foundation of China (21476267).

References and notes

1 S. S. Adav, M. Y. Chen, D. J. Lee and N. Q. Ren, *Chemosphere*, 2007, 67,1566-1572.

2 G. Busca, S. Berardinelli, C. Resiniand L. Arrighi, *J. Hazard. Mater.,*2008, 160, 265-288.

3 S. Ahmed, M. G. Rasul, W. N. Martens, R. Brownand M. A. Hashib, *Desalination,* 2010, 261,3-18.

4 D. Bahnemann, *Sol.Energy,* 2004,77, 445-459.

5 A. Kumarand D. Srinivas, *J. Mol. Catal. A: Chem.,* 2013,368-369, 112-118.

6 L.G. Devi, B. Nagarajand K.E. Rajashekhar, *Chem. Eng. J.,* 2012,181-182 , 259-266.

7 S.C. Xu, S.S. Pan, Y. Xu, Y. Y. Luo, Y. X. Zhang and G. H. Li, *J. Hazard. Mater.,* 2015, 283, 7-13.

8 A.D. Paola, S. Ikeda, G. Marcìand B. Ohtani, *Int. J. Photoenergy*, 2001, 3, 171-176.

9 M.V. Dozzi, S. Livraghi, E. Giamelloand E. Selli, *Photobio. Sci.,* 2011, 10, 343-349.

10 W. Yu, X.J. Liu, L.K. Pan, J. L. Li, J. Y. Liu, J. Zhang and P. Li, *Appl. Surf. Sci.*, 2014, 319, 107-112.

11 A.N. Kadam, R.S. Dhabbe and M.R. Kokate, *Spectrochim. Acta. A.*, 2014, 133, 669-676.

12 L. Liang, Y. Yulin, X. R. Liu,R. Q. Fan,Y. Shi and S. Li, *Appl. Surf. Sci.,* 2013, 265, 36-40.

13 HJ503-2009.Water quality-Determination of volatile phenolic compounds-4-AAP spectrophotometric method[S].

14D.Y. Zhao, J. Feng, Q. Huo, N. Melosh, G. H. Fredrickson, B. F. Chmelka and G. D. Stucky, *Science*,1998, 279, 548-552.

15 S.W. Patrick, W.W. Lukens and P.D. Yang, *Chem. Mater.,* 2000, 12, 686-696.

16 M.B. Emma, S. Fredrik and O. Magnus, *Langmuir,* 2013, 29, 13551-13561.

17 S. Khan, M. Al-Shahry and W.B. Ingler, *Science*, 2002, 297, 2243-2245.

18 J.C. Yu, J. Yu, W. Ho, Z. Jiang and L. Zhang, *Chem.mater.,* 2002, 14, 3808-3816.

19 D.G. Huang, S.J. Liao, S.Q. Quan, L. Liu, Z.J. He, J.B. Wan and W.B. Zhou, *J. Mater.Sci.*, 2007, 42, 8193-8202.

20 A.M. Czoska, S. Livraghi and M. Chiesa, *J. Phys. Chem. C*, 2008, 112, 8951-8956.

21 R. Asahi, T. Morikawa, T. Ohwaki and K. Aoki, *Science*, 2001, 293, 269-271.

22 J. J. Jiang, M. C. long, D. Y. Wu and W. M. Cai, *J. Phys. Chem.*, 2011, 7, 1149-1156.

23 P. V. Suraja, Z. Yaakob, N. N. Binitha, M. R. Resmi, and P. P.Silija, *Chem. Eng. J.*, 2011, 176, 265-271.

24 G.D. Yang, Z. Jiang, H.H. Shi, T.C. Xiao and Z.F. Yan, *J.Mater. Chem.*, 2010, 20, 5301-5309.

25 G. Yang, Z. Jiang, H. Shi and M.O. Jones, *Appl. Catal. B- Environ.*, 2010, 96, 458-465.

26 G.D. Yang, T. Wang, B.L. Yang, Z.F. Yan, S.J. Ding and T.C. Xiao, *Appl. Surf. Sci.*, 2013, 287, 135-142

27 C. Yan, K.F. Chen, C.H. Lai, S. W. Lai, Q. Chang and Y. P.Peng, *J. Environ. Sci.*,2014, 26, 1505-1512.

28 M. Sathish, B. Viswanathan and R. P. Viswanath, *Chem. Mater.*, 2005, 17, 6349-6353.

29 M. Mohai, I. Bertoti and M. Revesz, *Surf. Interface Anal.*, 1990, 15, 364-368.

30 J.M. Yu, Z.G. Liu and H.T. Zhang, *J.Environ. Sci.*, 2015, 28, 148-156.

31 W. Wang, C.H. Lu, Y.R. Ni, M.X. Su, W.J. Huang and Z.Z. Xu, *Appl. Surf. Sci.*, 2012, 258, 8696-8703.

32 Q.J. Xiang, K.L. Lv and J.G. Yu, *Appl. Catal. B- Environ.*, 2010, 96, 557-564.

33 J. Yu, W. Wang, B. Cheng and B.L. Su, *J. Phys. Chem. C.*, 2009, 113, 6743-6750.

34 D. Li, N. Ohashi, S. Hishita, T. Kolodiazhny and H. Haneda, *J.Solid State Electrochem.*, 2005, 178, 3293-3302.

35 S.Y. Yang, Y.Y. Chen, J.G. Zheng and Y.J. Cui, *J. Environ.Sci.*,2007, 19, 86-89.

Tables

Table 1 Pore structure character parameters of Ti-SBA-15 and non-metal (F, N)doped Ti-SBA-15

samples	BET area (m^2/g)	Mesopore volume (cm^3/g)	Average pore size (nm)
Ti-SBA-15	1004	1.38	5.49
N/Ti-SBA-15	730	1.07	5.34
F-N/Ti-SBA-15	719	1.58	14.21

Figure captions

Fig. 1 XRD pattern of N/Ti-SBA-15(N/Ti=2), F-N/Ti-SBA-15(F-N/Ti=2) and Ti-SBA-15(no doping)

Fig. 2 N_2 adsorption-desorption isotherm of Ti-SBA-15, N/Ti-SBA-15(N/Ti=2) and F-N/Ti-SBA-15(F-N/Ti=2)

Fig. 3 Pore size distribution of Ti-SBA-15, N/Ti-SBA-15andF-N/Ti-SBA-15

Fig. 4 UV-Vis DRS spectra of N/Ti-SBA-15 with different N content

Fig. 5 UV-Vis DRS spectra of F-N/Ti-SBA-15with different F-N content

Fig. 6 FT-IR patterns of Ti-SBA-15, N/Ti-SBA-15andF-N/Ti-SBA-15

Fig. 7 (A) Survey spectrum; (B) N1s XPS spectrum of the N/Ti-SBA-15, (C) Ti2p XPS spectra of Ti-SBA-15 and the N/Ti-SBA-15

Fig. 8 (A) Survey spectrum; (B) N1s XPS spectrum; (C) F1s XPS spectrum of the F-N/Ti-SBA-15, (D) Ti2p XPS spectra of Ti-SBA-15 and the F-N/Ti-SBA-15

Fig. 9 Photocatalysis degradation of phenol under ultraviolet (A) and visible light (B) in the presence of N/Ti-SBA-15

Fig. 10 Photocatalysis degradation of phenol under ultraviolet (A) and visible light (B) in the presence ofF-N/Ti-SBA-15

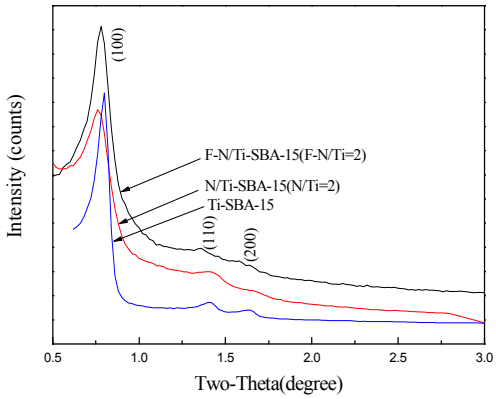

Fig. 1

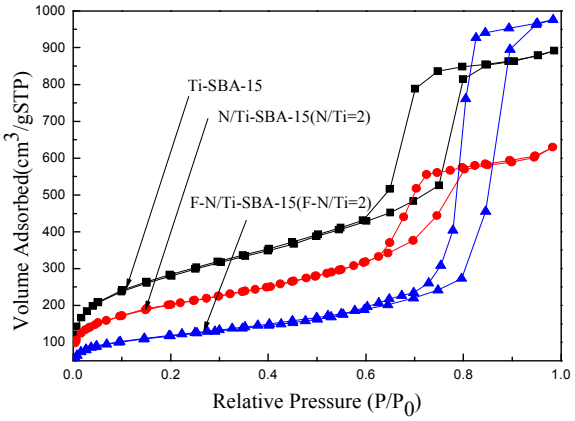

Fig. 2

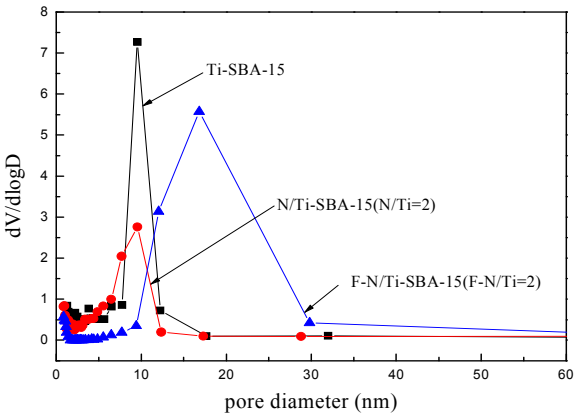

Fig. 3

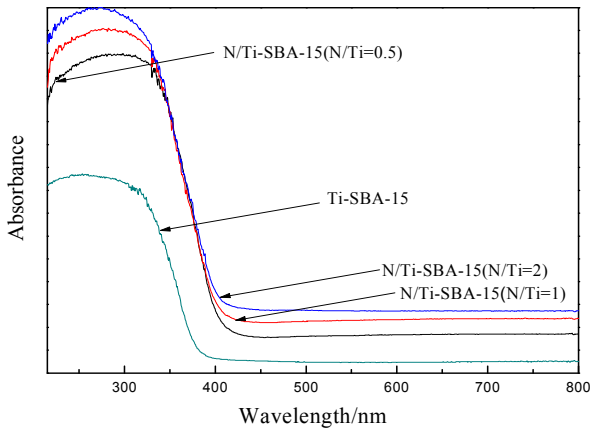

Fig. 4

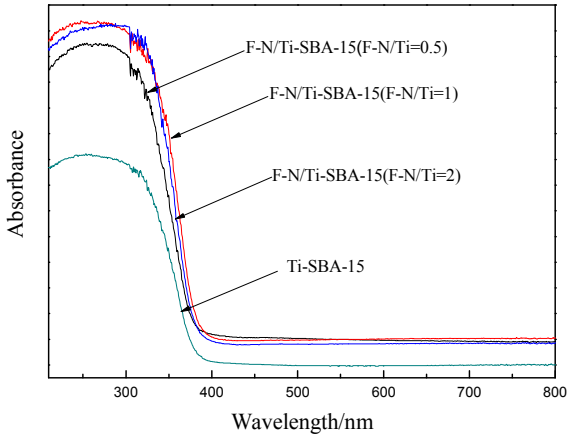

Fig. 5

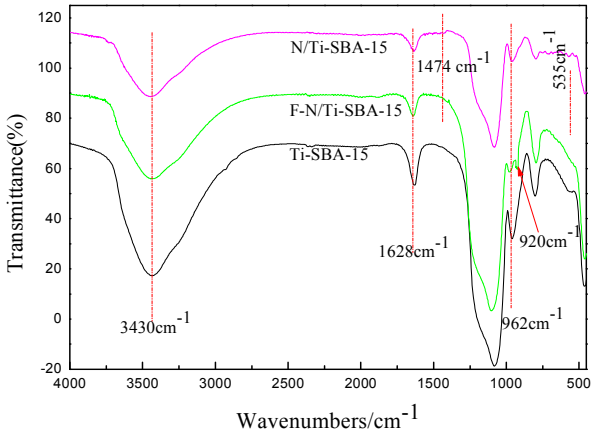

Fig. 6

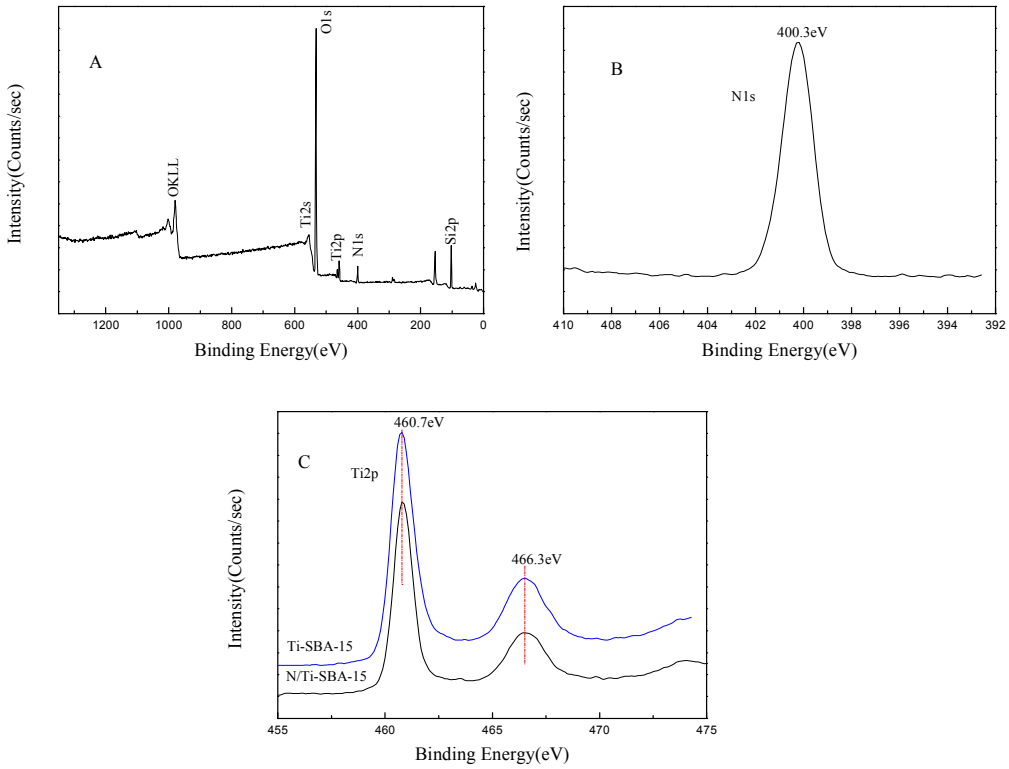

Fig. 7

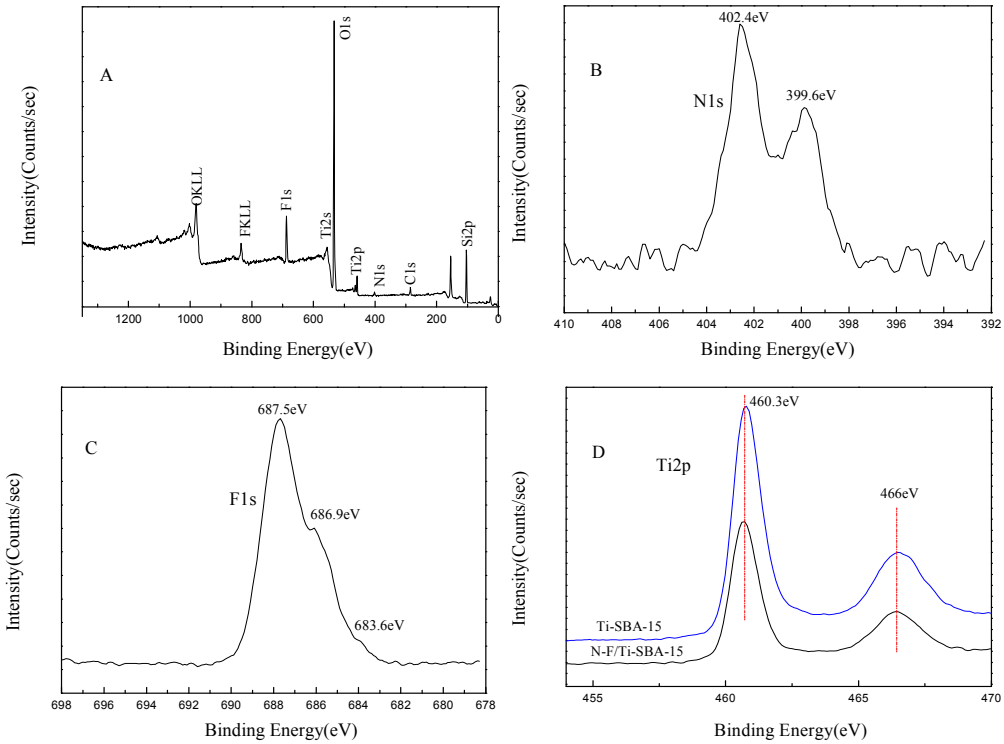

Fig. 8

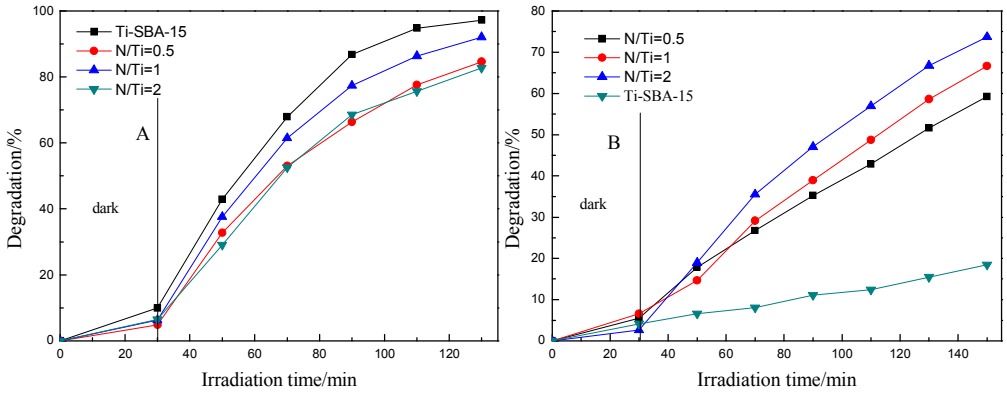

Fig. 9

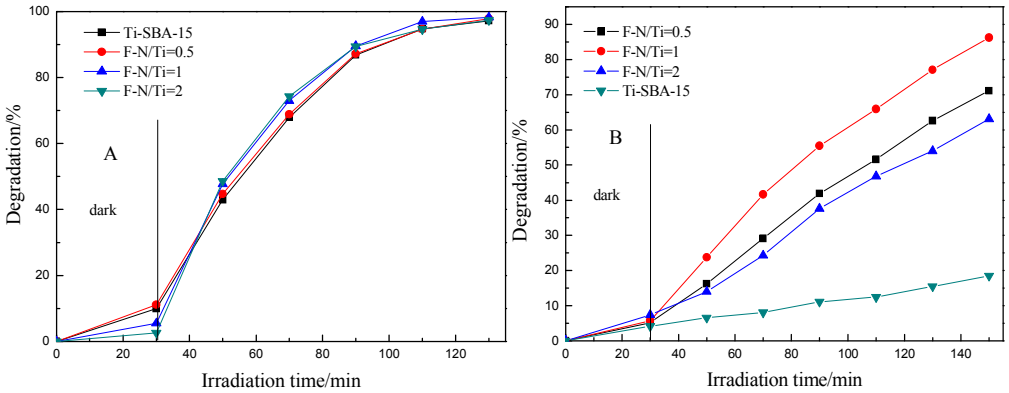

Fig. 10